Indian Journal of Chemistry
Vol. 63, November 2024, pp. 1141-1154
DOI: 10.56042/ijc.v63i11.12945

Ultrasound-assisted synthesis of 3,4-dihydropyrimidine-2(1*H*)-ones catalyzed by nanocomposites: An efficient and green approach

Reshma P Patil[a], Vilasrao A Kalantre[b], Dattatray K Pawar[c] & Krishna N Alasundkar*[a]

[a] Department of Chemistry, Government College of Engineering, Karad 415 124, Maharashtra, India

[b] Balasaheb Desai College, Patan 415 206, Maharashtra, India

[c] SIES College of Arts, Science and Commerce, Sion West, Mumbai 400 022, Maharashtra, India

E-mail: reshmapatil20591@gmail.com, korgchem@yahoo.co.in, kalantreva@yahoo.com, dkpawar2007@gmail.com

Received 2 August 2024; accepted (revised) 22 October 2024

ZnO NPs, CuO NPs, and ZnO-CuO NCs have been synthesized from aqueous extract of *Azadirachta indica* (neem plant) leaves extract by co-precipitation method in aqueous medium, under ultrasound irradiation. The traditional medicinal leaf extract of Neem (*Azadirachta indica*) in combination with ultrasound irradiation result in the formation of different morphologies of ZnO NPs, CuO NPs, and ZnO-CuO NCs. The significant antibacterial activity study of synthesized NPs has been carried out against two bacterial strains namely *E. coli* and *S. aureus* and it is shown that they have good ability to resist growth of bacteria. Among the synthesized nanoparticles bimetallic nanoparticles have drawn interest to a greater extent than monometallic nanoparticles. The enhancement could be due to the synergy between ZnO and CuO NPs. Hence, ZnO-CuO NCs used to productive synthesis of dihydropyrimidones derivatives under solvent-free technique is described. The environmental friendliness and reusability of the catalyst with steady activity, short reaction time, simple filtration process for separation of catalyst and simplified product isolation make this protocol attractive in organic synthesis.

Keywords: Nanocatalyst, Ultrasound irradiation, Multicomponent reaction, Antibacterial activity, Solvent-free technique, Green synthesis

Over the past decade, extensively evolvement has been acquired in the designing of green and sustainable approaches of organic transformation using Nanochemistry[1]. Therefore, upgrading eco-logical, effectual, and economic materials and invention techniques are essential[2]. Recently, researchers are prefering the use of nanostructured material-based catalysts as alternatives to conventional techniques. In comparable, the green synthesis of metal oxide NPs gained much attension from researchers due to its significant activities like low preparation cost, highly efficient and easily separable and recoverable, from the reaction mixture, low energy consumption and long life[3]. As a result of their properties and variability, metal oxides (ZnO, CuO, TiO_2, Fe_2O_3, NiO, CeO_2, ZrO_2, *etc*.) play a crucial role in catalysts[4,5]. Among the various available nanocatalysts ZnO NPs and CuO NPs nanocatalysts have inspired huge interest due to their frequent usability and sustainable nature. ZnO NPs, CuO NPs, ZnO-CuO NCs can be synthesized by various methods including co-precipitation, sol-gel, solvothermal, electro-spinning, photodeposition, micro-wave assisted, elctro-chemical, thermal-decomposition, and spray-pyrolysis[6-14]. Outoff these methods, simple co-precipitation method in aqueous medium under ultrasonication has several benefit in comparision to other convensional heating methods, such as simple, rapid reactions, avoid aggregation, uniform particle size distribution, immoderate yield and highly pure nanomaterials formed[15]. For ZnO NPs, CuO NPs, ZnO-CuO NCs synthesis, the most of the methods applied a various precursors and other reagents. Indeed, ZnO and CuO NPs, and ZnO-CuO NCs have found numerious applications in organic transformations as well as other fields *viz*. medicine, Solar cells, MCRs, photo-catalysis, *etc*. The green chemistry principles, promotes the use of cost-less, environmental-benign chemical substances, and waste-free methods that eliminate chemical waste[16]. Plant extracts contribute biomolecules which are safe and sound, green, cost-effective, and naturally available[17,18]. Thus, the alternate probable option for harsh chemicals is biomolecules[19]. Plant extract is used extensively in green and sustainable synthesis of metal oxide because it contains several biomolecules plays a key role as both reducing and stabilizing agents, which directly affects on the characteristics and morphologies of the resulting nanomaterials[2o,21]. According to previous literature survey, biomolecules based metal-oxide NP

synthesis involves three steps; formation of a biomolecule-metal ion complex, then a metal hydroxide complex, and ultimately metal-oxide nanoparticles[22,23].

As a green manner, ultrasonic irradiation has occupied much awareness for highly efficient and green synthesis of nanoparticles as compared to traditional approaches[24]. The neem (*Azadirachta indica*) leaf extract is a rich source of bioactive compounds; azadirachtin, nimbolide, gedunin, quinines, flavones, aldehydes, amides, organic acids, *etc*. owing cause the formation of zinc and copper ions to nanostructured ZnO NPs, CuO NPs and ZnO-CuO NCs[25]. From the previous reports; neem plant is recognized as a traditional tree in Indian ayurveda with its wide range of medicinal properties and it contains high concentration of zinc and copper ions. As well, it consist of reducing agents which performs as a capping and stabilizing agent[26,27]. Ultrasonication of aqueous plant extract produce quick dispersion of solute from the solvent and also enhance the rate of formation of nanoparticles[28]. From the principles of green methodology; the application of ultrasound technique has been fluently usable in organic synthesis because it is efficient and safe. The characteristic features of ultrasonication is the formation of cavitation takes-place due to the mechanical energy in the form of high frequency, high intensity, sound waves are irradiated resulting in the quick dispersion of NPs. In this present work; we are synthesized ZnO NPs, CuO NPs, and ZnO-CuO NCs and their antibacterial and catalytic study of synthesized nanoparticles[29]. We observe that, bimetallic nanoparticles have drawn a greater extent than monometallic nanoparticles due to presence of extra degree of freedom and coupling of one metal oxide with another metal oxide produce an enlarged surface area, and provide more reactive sites, greater surface area which increases their adsorption power and hence acts as efficient catalyst as compared to those of monometallic nanoparticles[3°]. Therefore, (ZnO-CuO) NCs exhibit higher activity as well as also used as a heterogenous Lewis acid catalyst. In the presence of Lewis acid enhance the rate of reaction. Therefore, we used ZnO-CuO NCs as a proficient catalyst for the solvent-free synthesis of bioactive 3,4-dihydropyrimidin-2(1H)-ones. Dihydropyrimidone derivatives have several biological and medicinal activities as calcium channel blocking activities, geroprotective, hepatoprotective, antitumour, antidiabetic activities, neuroprotectant, antioxidants[31].

In the present study, we analyzed the morphological study of ZnO NPs, CuO NPs and ZnO-CuO NCs synthesized from neem extract. An effortless and green access was modified to produce NPs. For this motive, an aqueous extract of neem (*Azadirachta indica*) leaves was used to synthesize ZnO NPs, CuO NPs and ZnO-CuO NCs through a rapid ultrasound-assisted process. Consequently labeled as ZnO-NE, CuO-NE, (ZnO-CuO)@[NE] NCs. The morphological study was carried out by XRD, SEM, EDX, FTIR, UV-Vis, BET techniques, antibacterial evaluation, *etc*. and the correlation between ZnO-NE, CuO-NE, (ZnO-CuO)@[NE] NCs was examined and we odserved that, bimetallic nanoparticles have several interesting properties such as, good crystalinity, larger surface area and tuning band gap energy due to the coupling of two different metal oxides, and highly antibacterial activity against bacteria namely *E. coli* and *S. aureus*; these properties justifies the efficiency of bimetallic (ZnO-CuO)@[NE] nanocomposite. In this present scenarios, the catalytic activities of (ZnO-CuO)@[NE] NCs were checked by introducing an economical recoverable catalyst for the synthesis of DHPM derivatives in solvent-free ultrasound-assisted route. Ultrasound irradiation route considered as a green and sustainable protocol also it enhance the rate of reaction as well as product yield in organic synthesis. So far DHPM synthesis has been done using metal oxide NPs, supported NPs but to my knowledge, based on literature review simple bimetallic coupling of (ZnO-CuO)@[NE] NCs have not been used for Biginelli reaction till date.

Experimental Section

Elegant and hygienic leaves of neem (*Azadirachta indica*) were obtained from Government College of Engineering campus; Karad, India. All chemicals employed in this study were the highest analytical grade (AR), available from local chemical suppliers and used as received. Deionized water (DW) was utilized throughout the experiment for solution preparation and washing activities. Melting points were determined on a open capillary and are uncorrected. Sonication was performed in Ultrasound apparatus BIO-TECHNICS-INDIA^{TM}. Ultrasonic bath (5.5L, 50 Hz frequency and nominal ultrasonic power of 150W). IR spectra were recorded on BRUKER ALPHA FT-IR Spectrometer with spectral range 375-7,500 cm^{-1}. Rigaku miniflex-600 operating with Cu kα radiation (λ=0.1540 nm) was used to acquire the Powder X-ray diffraction (XRD) of ZnO NPs, CuO NPs, ZnO-CuO NCs. The SEM and EDX analysis for morphological and

structural study of synthesized nanoparticles was carried out using a JEOL model JSM IT-200 accelerating voltage. ^{1}H NMR and ^{13}C NMR spectra were recorded on a Bruker AC (400 MHz for ^{1}H NMR and 100 MHz for ^{13}C NMR) spectrometer using DMSO as solvent and tetra-methylsilane (TMS) as an internal standard. The products were characterized by comparision of their spectral and melting points data with reference.

Preparation of neem plant extract (NE)

Garden-fresh leaves of neem (*Azadirachta indica*) were collected, cleaned in double-distilled water, air-dried, and then ground to fine powder by using grinder. 25 grams powder of neem leaves powder was immersed in 100 mL of double-distilled water and left to boil under ultrasonic irradiation at 60°C for 30 min. Then for separation of extract cooling and filtration was performed using (Whatman No. 42 filter paper). Finally; obtained greenish-yellow aqueous extract was stored in refrigerator for a further successive experiments for the synthesis of ZnO-NE NPs, CuO-NE NPs, and (ZnO-CuO)@[NE] NCs.

Synthesis of ZnO-NPs using neem plant extract (ZnO-NE)

ZnO, CuO and ZnO-CuO NCs were synthesized by the ultrasonic –assisted co-precipitation method using ($ZnSO_4.H_2O$), ($CuSo_4.5H_2O$) and neem leaves extract, following the reported procedure. To 50 mL of 0.05M solution of zinc sulphate monohydrate in deionized water, 25 mL of neem leaf extract was added dropwise to the solution for 1 h at 60°C under sonication. The *p*H of the mixture was then maintained at 10 by adding 1M NaOH drop by drop for 1 hr at 60°C under sonication. Sonication was continued for another 1 hr until pale yellow precipitate formed which indicates the formation of ZnO nanoparticles. Then the resulting solution was centrifuged, mother liquor was removed, precipitate was washed five times with deionized water, and then, precipitate was dried in air. The resulting solid was hand-crush by using pestle for transfering it to fine powder. Eventually, calcination of the powder was carried out in a muffle furnace at 200°C for 2h.

Synthesis of CuO-NPs using neem plant extract (CuO-NE)

TO 50 mL of 0.05 M solution of cupric sulphate pentahydrate in deionized water, 25 mL of neem leaf extract was slowly added to the solution for 1h at 60°C under sonication. The *p*H of the mixture was then maintained at 10 by adding 1M NaOH dropwise for 1hr at 60°C under sonication. Sonication was carried out for another 1 hr until lime green precipitate formed which indicates the formation of CuO NPs. Then solution was centrifuged, mother liquor was removed, precipitate was washed five times with deionized water, and then dried in air, calcination was carried out in a furnace at 150°C for 2h.

Synthesis of (ZnO-CuO) NCs using neem plant extract (ZnO-CuO)@[NE]

50% (ZnO-CuO)@[NE] NCs were synthesized by the ultrasound-assisted co-precipitation method. Typically, 50 mL of 0.05 M solution of zinc sulphate monohydrate and 50 mL of 0.05 M solution of cupric sulphate pentahydrate in deionized water, 50 mL neem leaf extract was introduced slowly drop by drop for 2h at 60°C under sonication. The *p*H of the mixture was then maintained at 10 by adding 1M NaOH dropwise for 2 hr at 60°C under sonication. Sonication was carried out for another 1 hr until dark green colour precipitate formed which indicates the formation of ZnO-CuO NCs. Then the solution was centrifuged, mother liquor was eliminated, precipitate was washed five times with deionized water and then precipitate was dried in air, calcination was carried out in a furnace at 150°C for 2h.

Synthesis of DHPM

A mixture of 1 mmol (0.102 g) benzaldehyde, 1 mmol (0.125 mL) ethyl acetoacetate, and 0.2 g of (ZnO-CuO)@[NE] NCs was stirred for 5min. Then, 1mmol (0.060g) Urea was added to reaction mixture and the mixture was kept under ultrasonic irradiations at ambient temperature. After completion of reaction, (monitored by TLC); a simple filtration process was used for complete separation of catalyst (ZnO-CuO)@[NE] NCs from the reaction mixture. The obtained product was recrystallized by ethanol. The recrystallized products were well identified by ^{1}H NMR and ^{13}C NMR.

Spectral data of some selected compounds

5-(Eth-oxycarbonyl)-4-phenyl-6-methyl-3,4-dihydropyrimidine-2(1*H*)-one (a): m.p.200°C (Lit: 201°C). FT-IR: 3307, 3207, 3071.23, 3017.55, 2883.37, 1729.83, 1639.27, 1454.78, 1371.44, 1219.21, 1086.68, 946.88, 876.72, 755.72, 694.44 cm^{-1}; ^{1}H NMR (DMSO-d_6, 400 MHz): δ 1.07 (t, 3H), 2.22 (s, 3H), 3.968 (q, 2H), 5.404 (s, 1H), 5.169 (d, 1H), 7.22 (d, 4H), 7.561 (s, 1H), 9.110 (s, 1H);

^{13}C NMR (DMSO-d_6, 100 MHz): δ 14.34, 18.22, 54.65, 59.53, 99.99, 126.70, 127.46, 128.47, 145.09, 148.26, 153.09, and 165.81; DEPT (DMSO-d_6, 100 MHz): δ 59.53.

5-(Ethoxycarbonyl)-6-methyl-4-(4-nitrophenyl)-3,4-dihdropyrimidine-2(1*H*)-one (b): m.p.204°C (Lit: 206°C). FT-IR: 3213.88, 3097.76, 2978.10, 1731.62, 1639.88, 1515.67, 1348.84, 1292.92, 1212.14, 1087.74, 774.29, 691.61 cm^{-1}; ^{1}H NMR (DMSO-d_6, 400 MHz): δ 1.093 (t, 3H), 2.236 (s, 3H), 3.978 (q, 2H), 5.283 (d,1H), 7.462 (d, 2H), 7.910 (s, 1H), 8.090 (d, 2H), 9.229 (s, 1H); ^{13}C NMR (DMSO-d_6, 100 MHz): δ 14.35, 18.33, 54.21, 59.69, 98.75, 123.73, 127.86, 147.01, 149.49, 152.56, 160.53, 165.47; DEPT (DMSO-d_6, 100 MHz): δ 59.69.

5-(Ethoxycarbonyl)-6-methyl-4-(4-chlorophenyl)-3,4-dihdropyrimidin-2(1*H*)-one (c): m.p.212°C (Lit: 215°C). FT-IR: 3230.03, 3115.03, 2976.33, 1699.53, 1643.79, 1598.34, 1481.67, 1368.93, 1287.99, 1218.29, 1085.62, 1008.66, 773.31 cm^{-1}; ^{1}H NMR (DMSO-d_6, 400 MHz): δ 1.11 (t, 3H), 2.22 (s, 3H), 3.972 (dd, 2H), 5.32 (s, 1H), 6.10 (s, 2H), 7.20 (m, 2H), 7.52 (m, 2H).

5-(Ethoxycarbonyl)-6-methyl-4-(2-nitrophenyl)-3,4-dihdropyrimidin-2(1*H*)-one (d): m.p.215°C (Lit: 217-220°C). FT-IR: 3283.15, 3120, 1735.06, 1663.09, 1587.59, 1516.85, 1363.40, 1137.81, 779.12 cm^{-1}; ^{1}H NMR (DMSO-d_6, 400 MHz): δ 0.8 (s, 1H), 1.3 (s, 1H), 2.1 (s, 3H), 2.3-2.4 (d, 2H), 3.8-4.2 (d, 5H), 5.5 (s, 1H), 6.5 (s, 1H), 7.4-7.5 (m, 2H), 7.8-7.9 (m, 4H).

5-(Ethoxycarbonyl)-6-methyl-4-(4-methoxyphenyl)-3,4-dihdropyrimidin-2(1*H*)-one (e): m.p.205°C (Lit: 203-207°C). FT-IR: 3385.31, 3020.25, 2967.85, 1739.76, 1573.22, 1429.70, 1368.01, 1218.21, 1098.34, 985.56, 885.62, 775.60, 602.43 cm^{-1}; ^{1}H NMR (DMSO-d_6, 400 MHz): δ 1.18 (t, 3H), 2.34 (s, 3H), 3.91 (s, 3H), 4.85 (dd, 2H), 5.54 (d, 1H), 5.96 (d, 2H), 6.84 (m, 2H), 7.25 (m, 2H).

Result and Discussion

Initially, ZnO-NE, CuO-NE, (Zn0-CuO)@[NE] NCs were prepared by using plant extract co-precipitation method. *Azadirachta indica* a scared medicinal plant leaves extract was used due to its phytochemical and pharmacological profile. The neem leaves extract is a rich source of bioactive compounds; azadirachtin, nimbolide, gedunin, quinines, flavones, aldehydes, amides, organic acids, *etc*. are water soluble[25]. The synthesized ZnO-NE NPs, CuO-NE NPs, (ZnO-CuO)@[NE] NCs were analyzed by FI-IR, UV-Vis, XRD, EDX, SEM, BET, antibacterial evaluation, *etc*. for their functional, structural, elemental, morphological, surface area analysis, and antibacterial study. On the basis of comparative study of synthesized nanoparticles; bimetallic coupling of (ZnO-CuO)@[NE] NCs have observed efficient properties than monometallic nanoparticles. Therefore, green synthesized (ZnO-CuO)@[NE] NCs were used as a catalyst for solvent-free Biginelli reaction under ultrasound irradiation.

Physical characterization

FT-IR analysis

Fig. 1(a) ZnO-NE, (b) CuO-NE, and (c) (ZnO-CuO)@[NE] NCs illustrate comparative FT-IR spectra of synthesized nanoparticles by using neem extract for

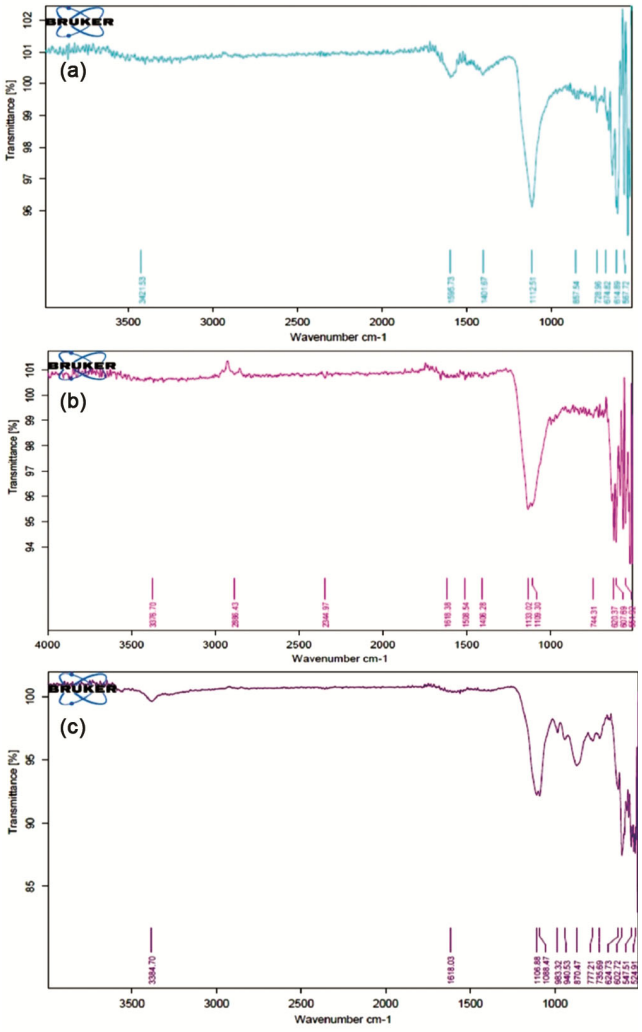

Fig. 1 — FT-IR of (a) ZnO-NE, (b) CuO-NE and (c) (ZnO-CuO)@[NE]

the identification of functional group and bonding information. The Zno-NE NPs shows a peak at around 1595 cm^{-1} and 1400 cm^{-1} plausibly due to C-H stretching vibration of $–CH_2$ group and vibration peaks for C=C and C=O bonds, respectively. The peaks around 1112 cm^{-1} and 857 cm^{-1} are due to the presence of C-N and C-Br stretch of amine and alkyl halide group respectively. The peak at 450 cm^{-1} indicates metal oxide bond. The CuO-NE NPs shows a peak around 1133 cm^{-1} and 1109 cm^{-1}due to C=C and C=O bonds[32]. The peak around 450 cm^{-1} indicates metal oxide bond. The (ZnO-CuO)@[NE] NCs shows 3384 cm^{-1} correlated to the bending and stretching vibration of the –OH of the surface adsorbed water molecules or hydroxyl groups in M-OH (M=Zn, Cu). The peaks around 1106 cm^{-1}, 1088 cm^{-1} and 870 cm^{-1} are due to C-H stretching vibration of $–CH_2$ group and vibration peaks for C=C and C=O bonds, and the presence of C-N and C-Br stretch of amine and alkyl halide group respectively. The peak around 450 cm^{-1} indicates metal oxide bond. The occupancy of extract associated bonds in correspondent bonds in all synthesized nanoparticles denotes neem extract acts as a capping and reducing agent.

X-ray Diffraction analysis

X-ray Diffraction (XRD) analysis gives the investigation about the crystalinity and phase purity of the synthesized material. The XRD pattern of the synthesized ZnO-NE Fig. 2(a) shows noticeable peaks positioned at 2θ values at 31.87°, 34.44°, 36.26°, 47.63°, 56.58°, 62.94°, 66.58°, 68.10°, 69.16°, 72.64°, 77.03°, corresponds to (100), (002), (101), (102), (110), (103), (200), (112), (201), (004) and (202) planes hexagonal ZnO-NE NPs which are agree with

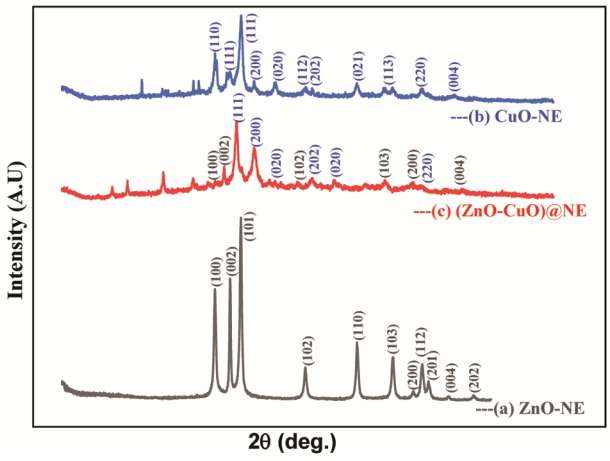

Fig. 2 — XRD of (a) ZnO-NE NPs, (b) CuO-NE NPs and (c) (ZnO-CuO)@[NE] NC

the standard reported (JCPDS 36-1451) values. The XRD pattern of the synthesized CuO-NE Fig. 2(b) shows noticeable peaks positioned at 2θ values at 32.47°, 35.50°, 38.69°, 38.89°, 46.19°, 48.66°, 56.64°, 61.46°, 68.00°, 72.92°, respectively, which corresponds to (110), (111), (111), (200), (020), (112), (202), (021), (113), (220), (004) planes of monoclinic CuO-NE NPs which are consistent with standard JCPDS reported values (JCPDS 01-080-1916) (Ref. 33). (ZnO-CuO)@[NE] NCs Fig. 2(c) observed at the 2θ values of 31.80°, 34.42°, 48.46°, 56.62°, 62.94°, 67.56°, 72.52° matched with the ZnO phase and those at the 2θ values of 35.50°, 37.7°, 46.19°, 48.66°, 56.64°, 68.00° matched with CuO phase confirming the formation of ZnO-CuO NCs. The sharp peaks with high intensity of the ZnO-NE, CuO-NE, and (ZnO-CuO)@[NE] NCs indicates high crystalinity. The particle size of synthesized NPs was calculated by Debye Scherrer formula (supporting information) and it is found 18.28 nm, 8.66 nm, 14.79 nm for ZnO-NE, CuO-NE, and (ZnO-CuO)@[NE] samples respectively. The obtained values indicated that the synthesized samples have crystallites in nanosize range. In view of possibility that catalytic efficiency could be improved by reducing the crystalline size, the nanosize range crystallites of the synthesized ZnO-CuO nanocomposite make the materials an attractive catalytic performance.

SEM and EDX analysis

Fig. 3 shows the SEM images for the surface analysis of size and morphology of plant extract synthesized ZnO-NE, CuO-NE, (ZnO-CuO)@[NE] NCs with different magnifications. Fig. 3[(a), (b), (c)] shows SEM of biosynthesized ZnO-NE NPs exhibit mushroom like mesophorous structure with diameter range 70-75 nm. While, Fig. 3[(d), (e), (f)] shows SEM of CuO-NE NPs having spherical shaped morphology with 55-60 nm diameter range. In Fig. 3[(g), (h), (i)] shows bio-synthesized (ZnO-CuO)@[NE] NCs posseses in cluster of spherical-like bright spot due to coupling of Zn and Cu ions with diameter range of 45-50 nm. In accordance with SEM results, the bimetallic nanocomposites were observed in smaller size than the monometallic metal oxides nanoparticles. Fig. 4. Demonstrate the energy dispersive spectroscopy EDS analysis was obtained at 20.0 kv HV accelerating voltage. The EDS spectrum of the sample confirmed the elemental composition of nanoparticles.

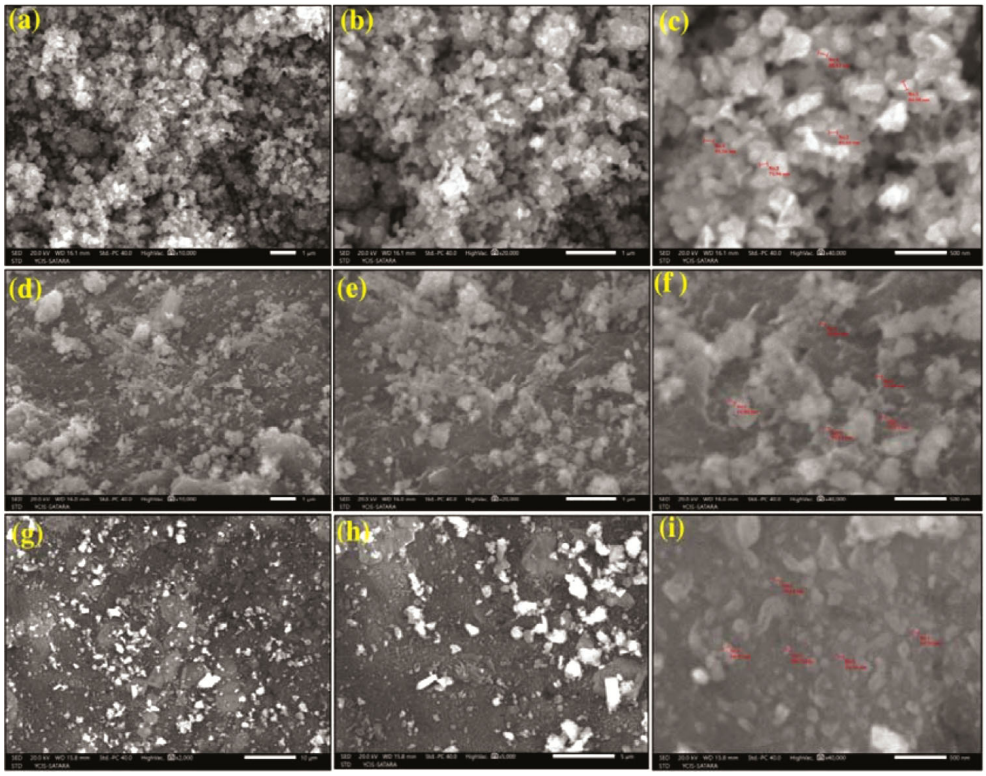

Fig. 3 — SEM images at different magnification of ZnO-NE NPs: a 10KX; b 20KX; c 40KX, CuO-NE NPs: d 10KX; e 20KX; f 40KX, (ZnO-CuO)@[NE] NC: g 2KX, h 10KX, i 40KX

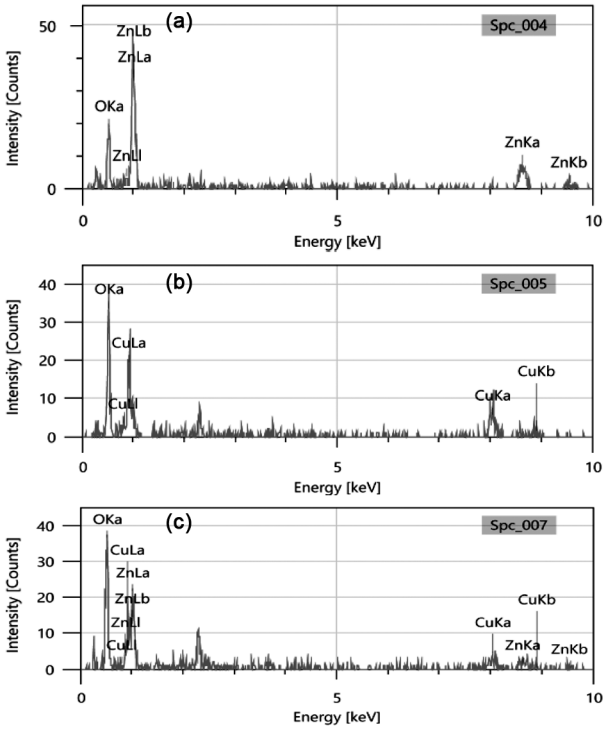

Fig. 4 — EDX of (a) ZnO-NE NPs, (b) CuO-NE NPs and (c) (ZnO-CuO)@[NE] NC

UV-Visible spectrometer

The study of optical properties of synthesized nanomaterials were studied by using UV-visible spectrometer in the range of 300-800 nm. The optical absorption spectrum of ZnO-NE, CuO-NE, (ZnO-CuO)@[NE] synthesized from neem extract is studied as shown in Fig. 5. The blueshift is observed in bio-derived nanoparticles due to its smaller particle size[34]. The upgraded photoactivity of synthesized particles further verified *via* concluding the band gap energies (Eg) calculated from Tauc's formula of each materials by plotting the graph of $(\alpha h\nu)^2$ *versus* $(h\nu)$ in Fig. 5. This competent valuation on the Eg of ZnO-NE, CuO-NE, (ZnO-CuO)@[NE] which were 3.28 eV, 2.93 eV, 2.74 eV respectively, and supported the results[35]. The results showed that the bandgap energy of the ZnO-CuO NCs is lower than ZnO and CuO NPs alone. Which enhanced efficiency of visible light-harvesting capacity makes ZnO-CuO NCs desirable candidate for photocatalytic applications.

BET-Surface area analysis

Fig. 6 recorded the effect of the extract on the surface characteristics of ZnO-NE, CuO-NE and

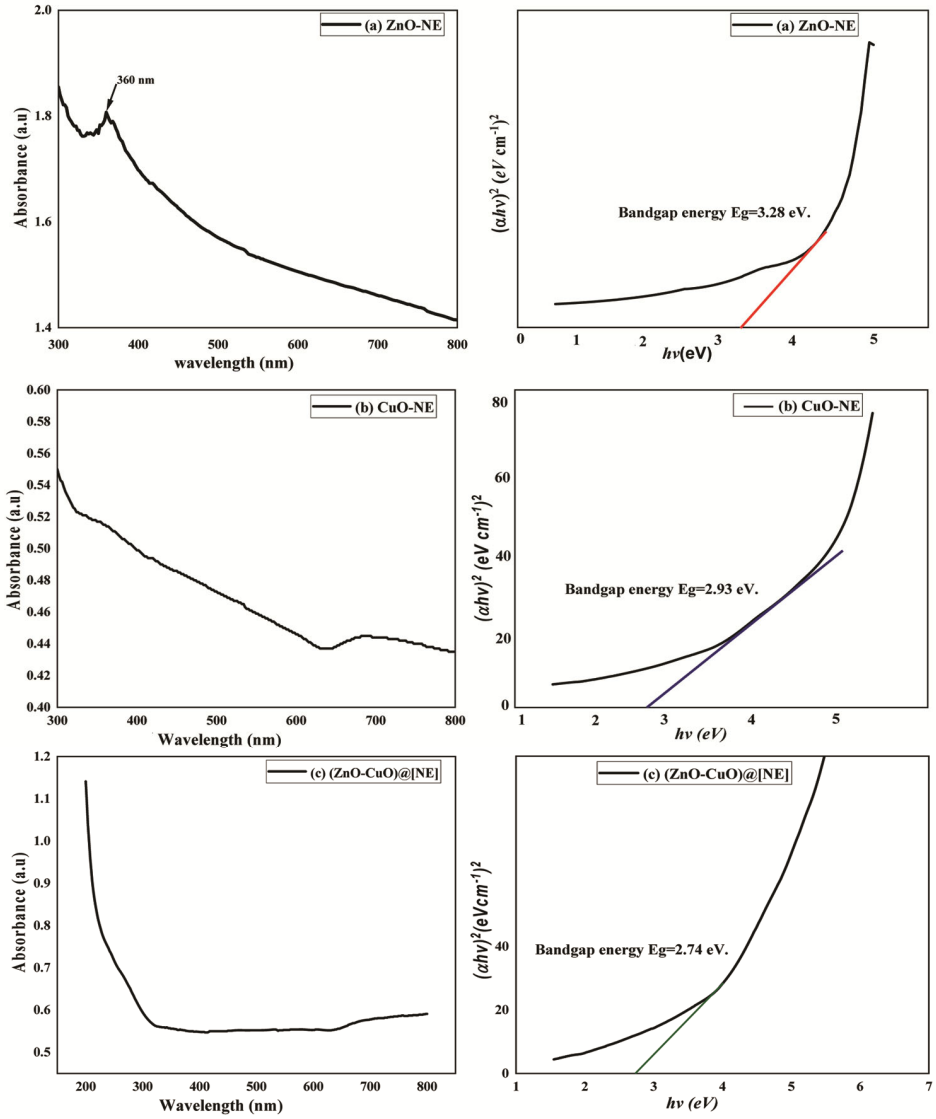

Fig. 5 — (a) ZnO-NE, (b) CuO-NE and (c) (ZnO-CuO)@[NE] optical absorption spectrum and Tauc's plot of $(\alpha hv)^2$ *versus* (hv) respectively

(ZnO-CuO)@[NE] , nitrogen adsorption-desorption trials. A wide distribution of pore and multilayer adsorption-desorption on the surface were obtained for ZnO-NE, CuO-NE and (ZnO-CuO)@[NE], as signified by the typical type III isotherm. According to the results, (ZnO-CuO)@[NE] acquired large BET surface area and pore volume relative to ZnO-NE, and CuO-NE alone; these BET surface areas are 17.248 $m^2\ g^{-1}$, 13.17 $m^2\ g^{-1}$, 6.3063 $m^2\ g^{-1}$ and pore volumes are 0.092657 $cm^3\ g^{-1}$, 0.1386 $cm^3\ g^{-1}$, and 0.044216 $cm^3\ g^{-1}$ respectively (Table 1). These results reveals that, the adsorption capacity of (ZnO-CuO)@[NE] will be higher than that of ZnO-NE, and CuO-NE. Simultaneously, the average pore size of (ZnO-CuO)@[NE] (2.76 nm) is smaller than that of ZnO-NE (81.6 nm) and CuO-NE (10.65 nm).

Antibacterial evaluation

Antibacterial activity of solvent extracts was determined by agar well diffusion method. In column containing 10^6 cfu/mL of each bacterial culture to be tested was spread on nutrient agar plates with sterile spreader. Subsequently, wells of 8 mm diameter were punched into the agar medium and filled with 100 µl of extract and allowed to diffuse at RT for 1 hour. The plates were then incubated in the upright position at 37° for 24 h. Wells containing the same volume distilled water served as negative controls while

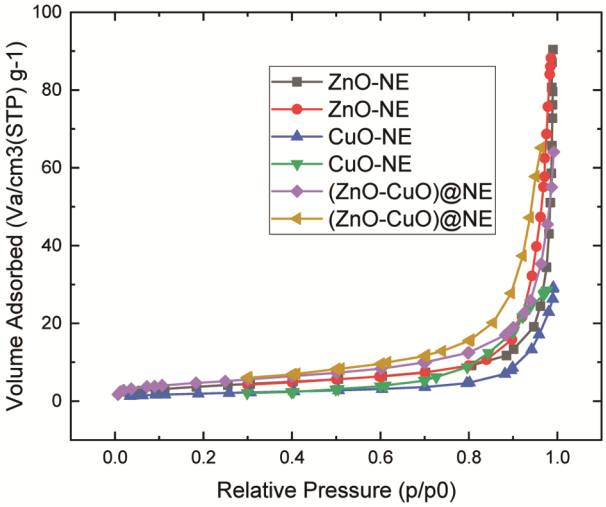

Fig. 6 — Isotherms of nitrogen adsorption-desorption of ZnO NPs, CuO NPs, and ZnO-CuO

Table 1 — Structural properties of samples (BET analysis)

Sample	BET surface area (m^2g^{-1})	Pore volume (cm^3g^{-1})	Average pore size (nm)
ZnO-NE	13.17	0.1386	81.6
CuO-NE	6.3063	0.044216	10.65
(ZnO-CuO)@[NE]	17.248	0.092657	2.76

standard antibiotic streptomycin were used as the positive controls. After incubation, the diameters of the growth inhibition zones were measured in mm. The significant antibacterial activity of synthesized NPs was carried out against bacteria namely *Escherichia. coli* and *Staphylococcus. aureus* and concluded that; they have a good ability to resist growth of bacteria. Among the synthesized nanoparticles bimetallic nanoparticles (Zno-CuO)@[NE] NCs was found to be highly active against *Escherichia coli* and *Staphylococcus aureus*[36,37]. The zone of inhibition for the synthesized compound has been mentioned in Fig. 7.

Catalytic applications

After successful validation of synthesized nanoparticles we observed bimetallic nanocomposites have drawn a greater extent than monometallic metal oxides nanoparticles. Therefore, we evaluated the effectiveness of ZnO-CuO NCs for the synthesis of dihydropyrimidone derivatives by using an equimolar amount of aldehyde, ethylacetoacetate, and urea (Table 1). First, we had studied Biginelli reaction without using catalyst and solvent under refluxed mode but we obtained less yield of product after 3h. This

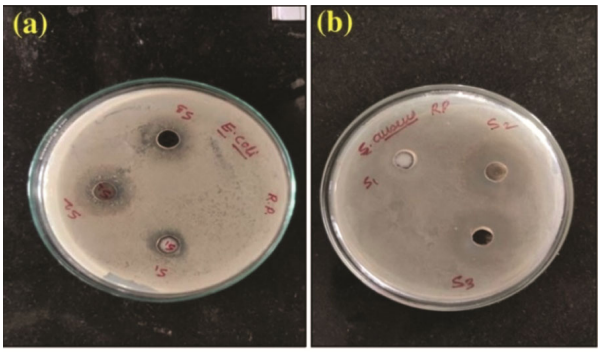

1) Antibacterial activity against *E. coli*-

Sample number	Sample 1	Sample 2	Sample 3
Zone of Inhibition (in mm)	14	16	22

2) Antibacterial activity against *S. aureus*-

Sample number	Sample 1	Sample 2	Sample 3
Zone of Inhibition (in mm)	10	20	21

Fig. 7 — Antibacterial evaluation of Sample 1 ZnO-NE NPs, Sample 2 CuO-NE NPs and Sample 3 (ZnO-CuO)@[NE] NC against bacteria (a) *E. coli* and (b) *S. aureus*

results clearly indicates the need of relevant catalyst to carry out reaction in green conditions. Then the yield was slightly improved when Lewis acid ($AlCl_3$, BF_3) was used as a catalyst in same condition. This results clearly denotes that, presence of Lewis acid enhance the rate and yield of reaction. Afterwords, instead of $AlCl_3$ Lewis acid we applied metal oxide; ZnO and CuO NPs separately synthesized by chemical method were used as a catalyst and EtOH as solvent and carry out reaction, both acts as Lewis acids. We observed that the yield rises under refluxed condition but reduce drastically at RT. These observation confirms, the necessity of the catalyst to increase the desired yield. Further, we screened the effect of the different solvents. In the presence of ethanol, methanol, AcOH, *etc*. poor yields were obtained; to follow green protocol, we turn our focus toward the reaction carry out by solvent-free technique. Therefore, we used green synthesized zinc oxide and copper oxide nanoparticles by using neem extract and run out reaction at RT then yield and speed of reaction slightly increased. From this, we have readily observed that there is need to changed the reaction condition, so we again carry out reaction by using ZnO-NE NPs and CuO-NE NPs separately under ultrasonication shows (65-75%) insignificantly progress in yield and it was due to aggregation of ZnO and CuO NPs. To avoid this aggregation and improving surface area we coupled these two metal oxides 50% (ZnO-

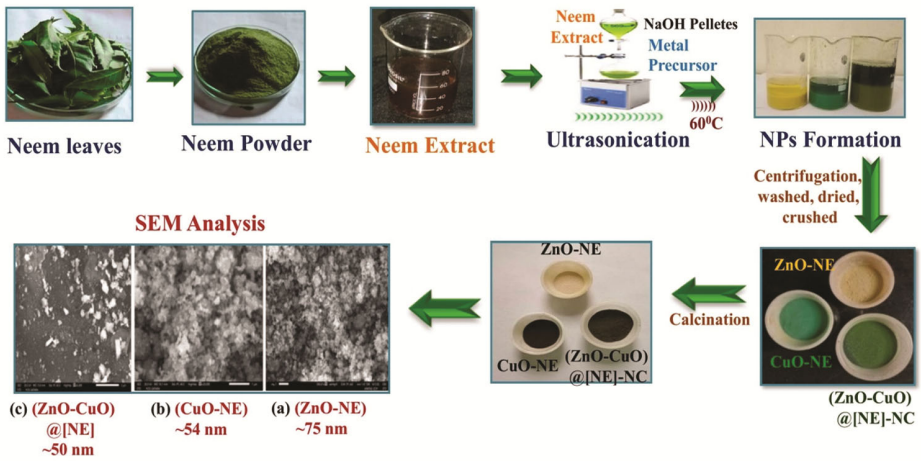

Scheme 1 — Ultrasound-assisted ZnO-NE, CuO-NE and (ZnO-CuO)@[NE] NCs synthesis using neem extract

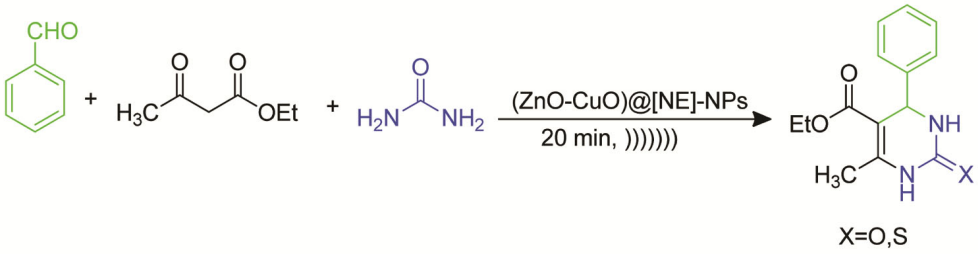

Scheme 2 — Synthesis of DHPMs (Biginelli reaction)

Table 2 — Screening of catalysts, solvents and reaction conditions

S. No.	Catalyst	Solvent	Conditions	Time	Yield (%)
1	–	–	Reflux	3 h	60
2	–	EtOH	Reflux	3 h	60
3	$AlCl_3$	EtOH	Reflux	3 h	65
4	BF_3	MeOH	Reflux	3 h	67
5	ZnO-NPs	EtOH	80°C, Reflux	2 h	75
6	CuO-NPs	EtOH	100°C	2 h	72
7	ZnO-NE NPs	EtOH	RT	2 h	70
8	CuO-NE NPs	EtOH	RT	2 h	67
9	ZnO-NE NPs	Solvent-free	RT,))))))	1 h	80
10	CuO-NE NPs	Solvent-free	RT,))))))	1 h	78
11	(ZnO-CuO)@[NE] NC	Solvent-free	RT,))))))	20-25 min	85-95

CuO) NCs and utilized in model reaction under ultrasonication and interestingly, we observed that reaction (Scheme 1) proceeded smoothly yielding the desired product in just 20-25 min. Screening the amount of catalyst was also determined by applying different amounts of catalyst (Table 2) to model reaction. This is probably due to the reason that (ZnO-CuO) NCs prepared from plant extract have mesophorous shape with good crystalinity and high surface area and tuning band gap energy due to the coupling also acts as strong Lewis acid, photocatalytic properties and redox-active material shows synergistic effect and results highly efficient reaction with high yield[38]. After optimized conditions, a series of DHPM were synthesized by reacting various substituted benzaldehyde with ethylacetoacetate and urea to check efficiency of this protocol (Scheme 2, Table 2). A plausible reaction mechanism for the Biginelli reaction is shown in Scheme 3.

Recyclability

Recyclability with high efficiency is the most important aspect of sustainability and waste reduction for any catalyst in organic transformation. The most

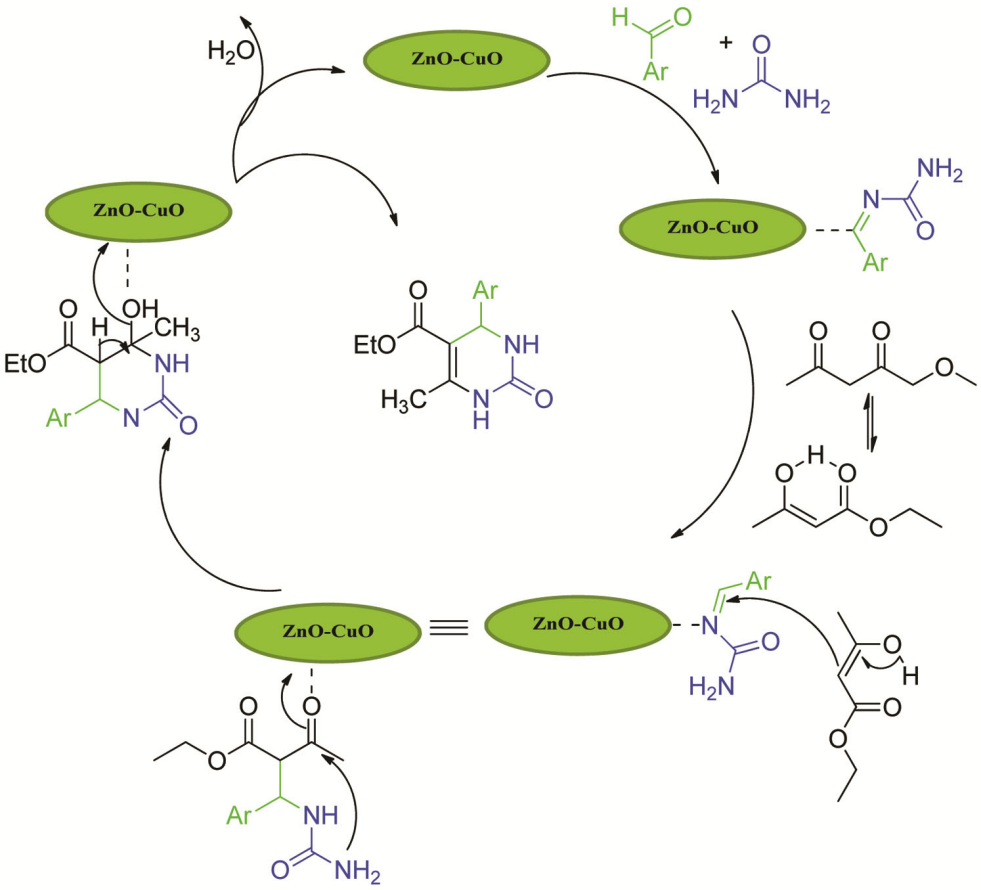

Scheme 3 — The plausible reaction mechanism for the Biginelli reaction

Table 3 — Impact of catalyst loading on the yield of reaction

S. No.	Catalyst	Amount of catalyst (g)	Time (min)	Yield (%)
1	50% (ZnO-CuO)@[NE] NC	0.05	40	70
2	50% (ZnO-CuO)@[NE] NC	0.10	30	75
3	50% (ZnO-CuO)@[NE] NC	0.15	20	85
4	50% (ZnO-CuO)@[NE] NC	0.20	20	94
5	50% (ZnO-CuO)@[NE] NC	0.25	20	90

Reaction condition: Aldehyde (1 mmol), Ethyl acetoacetate (1 mmol), and Urea (1 mmol)

important significance of this (ZnO-CuO)@[NE] heterogenous nanocomposites with respect to previously reported work. To check the catalyst sustainability in retaining its activity (ZnO-CuO)@[NE] NC (catalyst) were separated by a simple filtration process after completion of the reaction and recycled without significant loss in its catalytic properties and then washed with ethanol/water treatment and drying (Table 3, Table 4, Table 5). Further, it was then subjected to the next catalytic cycles and found to be active without an appreciable reduction in the product yield which confirmed that the (ZnO-CuO)@[NE] NC having enough stability and can be reused up to four consecutive runs (Fig. 8). Afterwords, in order to examine the steadiness of ZnO-CuO NC during four runs, the SEM and XRD pattern of the fresh ZnO-CuO NCs was compared with the recovered one after the fourth cycle SEM and XRD spectra obtained (Fig. 9). The recovered catalyst were found to be almost similar to the fresh one without much loss in its surface and structural morphology. The leaching of the catalyst was not seen even though it was recycled many times, are the green features of this study.

Table 4 — (ZnO-CuO)@[NE] NCs catalysed Biginelli reaction of ethyl acetocatate, urea and different benzaldehydes

Entry	Aldehyde	Product	Reaction Time (min)	Overall yield (%)	m.p. (°C) Obsd. (Theo.)
a	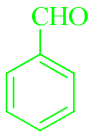	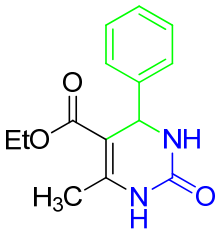	20	95	200 (201)
b	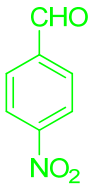	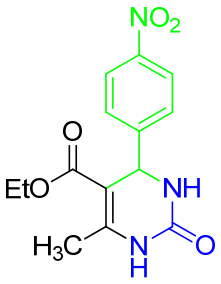	25	92	204 (206)
c	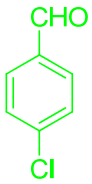	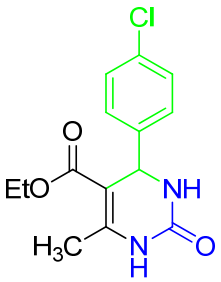	20	90	212 (215)
d	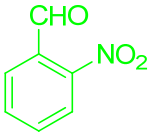	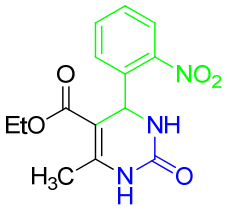	20	87	210 (212)
e	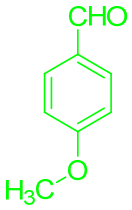	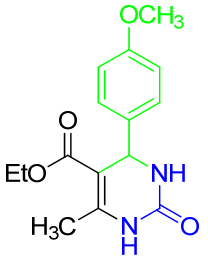	25	89	200 (201)
f	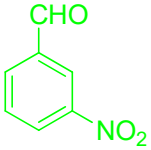	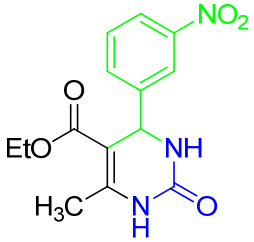	25	85	225 (227)

(*Contd.*)

Table 4 — (ZnO-CuO)@[NE] NCs catalysed Biginelli reaction of ethyl acetocatate, urea and different benzaldehydes

Entry	Aldehyde	Product	Reaction Time (min)	Overall yield (%)	m.p. (°C) Obsd. (Theo.)
g	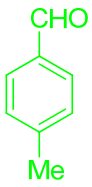	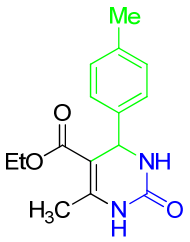	22	90	206 (208)
h	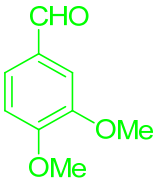	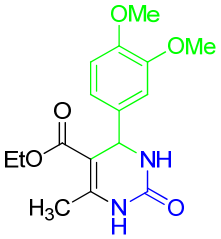	30	89	170 (175)
i	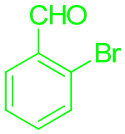	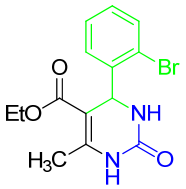	20	86	206 (208)

Reaction condition: (1 mmol) aldehyde, (1 mmol) ethylacetoacetate, and (1 mmol) urea and 0.20 g ZnO-CuO)@[NE] NC.

Table 5 — Comparison of present work with the latest published works for DHPM synthesis

S. No.	Catalyst	Condition	Time	Yield (%)	[Lit. Ref.]
1	$ZnCl_2$	AcOH, RT	2 h	85	[39]
2	La_2O_3	EtOH,))))))	30-80 min	90-97	[40]
3	Fe_2O_3 NPs	–	–	93-96	[41]
4	$Sr_2As_2O_7$	Solvent-free, 90°C	100 min	44-96	[42]
5	Nano-Fe-ZnO	EtOH, reflux	–	90-96	[43]
6	NiO NPs	Solvent-free, 90°C	90 min	72-97	[44]
7	Fe_3O_4@SiO_2-$ZnCl_2$	80°C, EtOH	1-2.5 h	90-95	[45]
8	ZnO NPs	80°C, Methanol	60 min	87	[46]
9	CuO NPs	90°C	90 min	95	[47]
10	(ZnO-CuO)@[NE] NC	Solvent-free,)))))	20-25 min	85-95	[Present work]

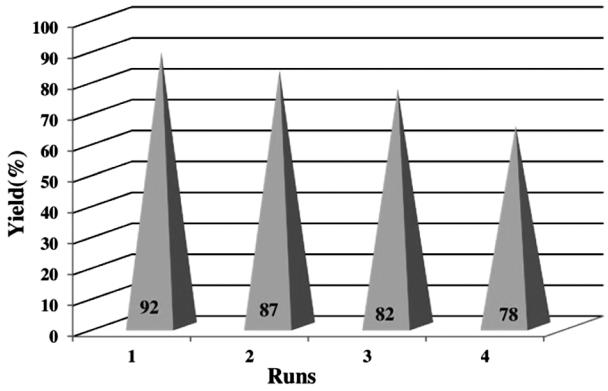

Fig. 8 — Effect of number of runs of (Zn0-CuO)@[NE] NCs on yield of DHPMs

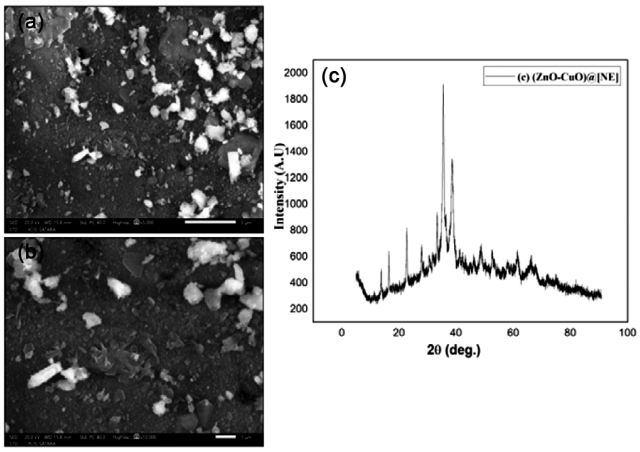

Fig. 9 — SEM and XRD of (Zn0-CuO)@[NE] NCs after fourth run

Conclusion

Ultrasound-assisted bio-derived ZnO NPs, CuO NPs, and ZnO-CuO NC have been successfully synthesized by simple co-precipitation method using neem extract. The synthesized samples was characterized by various techniques. The analysis results reveals that the improved performance of bimetallic hetero ZnO-CuO NC relative to ZnO and CuO NPs. The enhancement could be due to the synergy between ZnO and CuO NPS, resulting improved catalytic efficiency due to its good crystalinity, surface area and tuning band gap energy. Thus, the bimetallic nanocomposites ZnO-CuO NC prepared using neem extract could make the material a desirable catalyst for the bioactive Biginelli reaction under ultrasound irradiation and solvent-free technique has been developed. Simple preparation method, easiness separation of catalyst from the reaction mixture by effortless filtration method is the main superiority of this catalytic system. Environmental-benign route, Green catalyst, easy separation, reusable catalyst, ultrasound-assisted and solvent-free technique, short reaction time, atom-efficiency, *etc*. which makes this study attractive in organic synthesis and pursue strictly green and sustainable protocol.

Supplementary Information

Supplementary information is available in the website http://nopr.niscpr.res.in/handle/123456789/58776.

Acknowledgements

One of authors, R. P. Patil gratefully acknowledges support from Chhatrapati Shahu Maharaj Research, Training and Human Development Institute (SARTHI), Government of Maharashtra for providing the Chhatrapati Shahu Maharaj National Research Fellowship, India (CSMNRF-2021). R. P. Patil thanks the Government College of Engineering, Karad (Autonomous) for providing research facilities and laboratory and also thanks the Balasaheb Desai College, Patan, for partial support.

Author contributions

Reshma P. Patil: Conceptualization, Methodology, Investigation, Formal analysis, Writing-original draft. Dattatray K. Pawar: Data curation. Krishna N. Alasundkar: Implementation of data, Editing of the manuscript, Project administration. Vilasrao A. Kalantre: Guidance, and Supervision.

Funding

Chhatrapati Shahu Maharaj National Research Fellowship (CSMNRF-2021), Government of Maharashtra, India.

Conflict of Interest

There are no conflicts of interest to declare.

References

1 Varma R S, *ACS Sus Chem Eng*, 4 (2016) 5866.
2 Ibrahim R K, Hayyan M, AlSaadi M A, A. Hayyan, S. Ibrahim, *Env Sci Poll Res*, 23 (2016) 13754.
3 Tahmasbi M, Koukabi N & Armandpour O, *Hetero Comm*, 28 (2022) 1.
4 Velempini T, Prabakaran E & Pillay K, *Mat Today Chem*, 19 (2021) 100380.
5 Danish M S S, Estrella L L, Alemaida I M A, Lisin A, Moiseev N, Ahmadi M, Nazari M, Wali M, Zaheb H & Senjyu T, *Metals*, 11 (2021) 80.
6 Velayi E & Norouzbeigi R, *Ceramics Int*, 45 (2019) 16864.
7 Vo N L U, Nguyen T T. V, Nguyen T, Nguyen P A, Nguyen V M, Nguyen N H, Tran V L, Phan N A & Huynh K P H, *J Nanomat*, 2020 (2020) 1.
8 Podrojková N, Patera J, Popescu R, Škoviera J, Oriňaková R & Oriňak A, *Chem Sel*, 6 (2021) 4256.
9 Fan C, Sun F, Wang X, Majidi M, Huang Z, Kumar P & Liu B, *J Mater Sci*, 55 (2020) 7702.
10 Zhang J, Gao S, Wang G, Ma X, Jiao S, Sang D, Liu S, Mao M, Fang H & Wang J, *Eur J Inorg Chem,* 2019 (2019) 2654.
11 Pardakhty A, Ranjbar M, Moshafi M H & Abbasloo S, *J Clust Sci,* 29 (2018) 1061.
12 Nur A, Rofi'uddien J, Basir M A, Nazriati N & Fajaroh F, *J Chem Eng*, 2 (2018) 59.
13 Saravanan R, Karthikeyan S, Gupta V K, Sekaran G, Narayanan V & Stephen A, *Mat Sci Eng*, C 33 (2013) 91.
14 Saravanakkumar D, Sivaranjani S, Kaviyarasu K, Ayeshamariam A, Ravikumar B, Pandiarajan S, Veeralakshmi C, Jayachandran M & Maaza M, *J Semicond*, 39 (2018) 033001.
15 Sharifi M, Pothu R & Boddula R, *Green Sustainable Process for Chemical and Environmental Engineering and Science*,

(Elsevier) 2021, p. 315. (https://doi.org/10.1016/B978-0-12-819848-3.00007-4)
16 Paristiowati M, Zulmanelis Z & Nurhadi M.F, *J Tadris Kimiya*, 4 (2019) 11.
17 Ali S G, Ansari M A, Jamal Q M S, Almatroudi A, Alzohairy M A, Alomary M N, Rehman S, Mahadevamurthy M, Jalal M, Khan H M, Adil S F, Khan M & Al-Warthan A, *Arabian J Chem,* 14 (2021) 103044.
18 Adil S F, Assal M E, Khan M, Al-Warthan A, Siddiqui M R H & Liz-Marzán L M, *Dalton Trans*, 44 (2015) 9709.
19 Nasrollahzadeh M, Sajjadi M, Sajadi S M & Issaabadi Z, *Elsevier*, 28 (2019) 145.
20 Marslin G, Siram K, Maqbool Q, Selvakesavan R, Kruszka D, Kachlicki P & Franklin G, *Materials*, 11 (2018) 940.
21 Khan M, Shaik M.R, Adil S.F, Khan S.T, Al-Warthan A, Siddiqui M R H, Tahir M N & Tremel W, *Dalton Trans*, 47 (2018) 11988.
22 Azizi S, Mohamad R, Bahadoran A, Bayat S, Rahim R A, Ariff A, Saad W Z, *J Photochem Photobio B: Bio*, 161 (2016) 441.
23 Bayrami A, Parvinroo S, Habibi-Yangjeh A & Pouran S R, *Nanomed Biotech*, 46 (2018) 730.
24 Maleki A, *Ultrason Sonochem*, 28 (2017) 115.
25 Bhuyan T, Mishra K, Khanuja M, Prasad R & Varma A, *Mat Sci Semicon Proc*, 32 (2015) 55.
26 Nath D & Banerjee P, *Env Toxi Pharm*, 33 (2013) 997.
27 Islas J.F, Acosta E, Buentello Z G, Delgado-Gallegos J L, Moreno-Treviño M G, Escalante B & Moreno-Cuevas J E, *J Funct Foods,* 74 (2020) 104171.
28 Bayrami A, Alioghli S, Pouran S.R, Yangjeh A H, Khataee A & Ramesh S, *Ultrason Sonochem*, 55 (2019) 57.
29 Basavegowda N, Somu P, Shabbirahmed A M, Gomez L A & Thathapudi J J, *Photochem Photobiol Sci*, 21 (2022) 1357.
30 G. Sharma, A. Kumar, S. Sharma, Mu. Naushad, R. Prakash Dwivedi, Alothman Z A & Mola G T, *J King Saud Uni Sci*, 31 (2019) 257.
31 Naik T R R, *Intech Open*, 2020. (https://doi.org/10.5772/intechopen.89860)
32 Banakar S H, Dekamin M G & Yaghoubi A, *New J Chem*. 42, (2018), 14246 .
33 Sharmila G, Pradeep R S, Sandiya K, Santhiya S, Muthukumaran C, Jeyanthi J, Kumar N M & Thirumarimurgan M, *J Mol Struct*, 1165 (2018) 288.
34 Shinde B, Kamble S, Gaikwad P, Ghanwat V, Tanpure S, Pagare P, Karale B & Burungale A, *Res Chem Inter*, 44 (2018) 3097.
35 Bekru A G, Tufa L T, Zelekew O A, Goddati M, Lee J & Sabir F K, *Omega*, 7 (2022) 30908.
36 Sankpal S A, M B Deshmukh, P V, Anbhule D K, Salunkhe K N, Alsundkar P P, Patil D R, Chandam S D, Jagadale A G, Mulik S S & Rokade, *J Chem Pharm Res*, 2 (2010) 574.
37 Deshmukh M B, Alasundkar K N, Salunkhe S M, Salunkhe D K, Sankpal S A, Patil D R & Anbhule P V, *Indian J Chem*, 47B (2008) 1915.
38 Patil R P, V A Kalantre & Alasundkar K N, *Res Chem Intermed*, 49 (2023) 5163.
39 Thorat B R, Gurav A, Dalvi B, Sawant A, Lokhande V & Mali S N, *Curr Chinese Chem*, 1 (2021) 30.
40 Adole VA, Pawar T B, Koli P B & Jagdale B S, *J Nanostruc Chem*, 9 (2019) 61.
41 Sanap D, Avhad L, Ghotekar S & Gaikwad N D, *J Mol Struct*, 1283 (2023) 135246.
42 Esmaeili R, Kafi-Ahmadi L & Khademinia S, *J Mol Struct*, 1216 (2020) 128124.
43 Waghchaure R H, Jagdale B S, Koli P B & Adole V A, *J Indian Chem Soc*, 99 (2022) 100468.
44 Khashaei M, Kafi-Ahmadi L, Khademinia S, Poursattar Marjani A & Nozad E, *Sci Rep*, 12 (2022) 8585.
45 Rahimi S & Soleimani E, *Results Chem*, 2 (2020) 100060.
46 Moumita Saha & Das A R, *Curr Green Chem*, 7 (2020) 53.
47 Alinezhad H & Pakzad K, *Org Prep Proced Int*, 52 (2020) 319.